

PAPER • OPEN ACCESS

Solid lipid nanoparticles as a vehicle for brain-targeted drug delivery: two new strategies of functionalization with apolipoprotein E

To cite this article: Ana Rute Neves *et al* 2015 *Nanotechnology* **26** 495103

View the [article online](#) for updates and enhancements.

You may also like

- [Fabrication, characterization and optimization of artemether loaded PEGylated solid lipid nanoparticles for the treatment of lung cancer](#)
Hiren Khatri, Nimit Chokshi, Shruti Rawal *et al.*
- [The effect of cetyl palmitate crystallinity on physical properties of gamma-oryzanol encapsulated in solid lipid nanoparticles](#)
Uracha Ruktanonchai, Surachai Limpakdee, Siwaporn Meejoo *et al.*
- [Preparation of oridonin-loaded solid lipid nanoparticles and studies on them *in vitro* and *in vivo*](#)
Dianrui Zhang, Tianwei Tan and Lei Gao



ECS
The
Electrochemical
Society
Advancing solid state &
electrochemical science & technology

DISCOVER
how sustainability
intersects with
electrochemistry & solid
state science research

Solid lipid nanoparticles as a vehicle for brain-targeted drug delivery: two new strategies of functionalization with apolipoprotein E

Ana Rute Neves^{1,5}, Joana Fontes Queiroz^{1,5}, Babette Weksler²,
Ignacio A Romero³, Pierre-Olivier Couraud⁴ and Salette Reis¹

¹REQUIMTE, Department of Chemical Sciences, Faculty of Pharmacy, University of Porto, Rua de Jorge Viterbo Ferreira, 228, 4050-313 Porto, Portugal

²Division of Hematology—Medical Oncology, Weill Cornell Medical College, New York, NY 10065 USA

³Department of Biological Sciences, The Open University, Walton Hall, Milton Keynes, MK7 6AA, UK

⁴Institut Cochin, Centre National de la Recherche Scientifique, UMR 8104, Institut National de la Santé et de la Recherche Médicale (INSERM) U567, Université René Descartes, Sorbonne Paris Cité, Paris, France

E-mail: shreis@ff.up.pt

Received 29 July 2015, revised 23 September 2015

Accepted for publication 12 October 2015

Published 17 November 2015



CrossMark

Abstract

Nanotechnology can be an important tool to improve the permeability of some drugs for the blood–brain barrier. In this work we created a new system to enter the brain by functionalizing solid lipid nanoparticles with apolipoprotein E, aiming to enhance their binding to low-density lipoprotein receptors on the blood–brain barrier endothelial cells. Solid lipid nanoparticles were successfully functionalized with apolipoprotein E using two distinct strategies that took advantage of the strong interaction between biotin and avidin. Transmission electron microscopy images revealed spherical nanoparticles, and dynamic light scattering gave a Z-average under 200 nm, a polydispersity index below 0.2, and a zeta potential between -10 mV and -15 mV. The functionalization of solid lipid nanoparticles with apolipoprotein E was demonstrated by infrared spectroscopy and fluorimetric assays. *In vitro* cytotoxic effects were evaluated by MTT and LDH assays in the human cerebral microvascular endothelial cells (hCMEC/D3) cell line, a human blood–brain barrier model, and revealed no toxicity up to 1.5 mg ml⁻¹ over 4 h of incubation. The brain permeability was evaluated in transwell devices with hCMEC/D3 monolayers, and a 1.5-fold increment in barrier transit was verified for functionalized nanoparticles when compared with non-functionalized ones. The results suggested that these novel apolipoprotein E-functionalized nanoparticles resulted in dynamic stable systems capable of being used for an improved and specialized brain delivery of drugs through the blood–brain barrier.

 Online supplementary data available from stacks.iop.org/NANO/26/495103/mmedia

⁵ These authors have contributed equally to this work.



Content from this work may be used under the terms of the Creative Commons Attribution 3.0 licence. Any further distribution of this work must maintain attribution to the author(s) and the title of the work, journal citation and DOI.

Keywords: blood-brain barrier, drug-delivery, nanotechnology, solid lipid nanoparticles, active-targeting, functionalization, apolipoprotein E

1. Introduction

The blood–brain barrier (BBB) is an almost impermeable, highly selective and dynamic specialized barrier system of capillary endothelial cells that protects the brain against pathogenic organisms and unwanted and harmful substances while supplying the brain with the needed nutrients for proper function [1–3]. It is well known that only lipid-soluble small molecules with a molecular weight of about 450 daltons can cross the BBB by passive diffusion, which reduces the number of drugs that can enter the central nervous system (CNS) in the drug market to less than 2% of all potential drug candidates [4, 5]. In addition, several membrane transporters located in the barrier mediate molecular efflux from the CNS compartment back to the blood. P-glycoprotein (P-gp) is probably the most studied and characterized system involved in the cellular efflux of a broad range of drugs [6, 7]. For this reason, the conventional drug delivery systems that release a drug into the systemic circulation fail to deliver it effectively to the brain; therefore there is a huge need to develop and design approaches with a specific target to the brain in a better and more effective way for the treatment of brain diseases [7, 8]. Since the 1990s solid lipid nanoparticles (SLNs) have shown to be very promising for drug delivery in the brain. These spherical particles are composed of biodegradable and biocompatible excipients and are produced from solid lipids with melting points higher than body temperature, remaining in a solid state after administration [1, 9]. Thereby, lipid-based nanocarriers hold strong promise to the delivery of drugs directly to the brain because of their lipid nature (lipophilicity) and small size, which gives the SLNs a natural tendency to cross the BBB; their very low cytotoxicity, shown *in vitro*; and because they can easily avoid the P-gp efflux activity at brain endothelial cells (especially when coated with polysorbate 80) [6, 10–14]. Moreover, opsonization by plasma proteins can also be reduced by providing a hydrophilic coating with polysorbates and polyethylene glycol (PEG), which results in an increased blood circulation time and thus a higher chance to be taken up by the brain [1]. Polysorbate 80 can also be used to prepare nanoparticles with improved brain-specific delivery due to the high affinity to adsorb plasma apolipoproteins on the surface, followed by low-density lipoprotein (LDL) receptor recognition and uptake by endothelial cells lining brain capillaries [15–17]. Actually, apolipoproteins such as Apolipoprotein E (Apo E) have been employed already in albumin nanoparticles for targeting LDL receptors at the BBB [18, 19]. Especially, Apo E Receptor 2 appears to be predominantly expressed in the brain, and it is known that these receptors bind Apo E with high affinity [20–22]. Hence, Apo E-coupled nanoparticles may mimic lipoprotein particles (like LDL) that are endocytosed into the BBB endothelium and transcytosed through the BBB endothelium into the brain [23, 24]. However, none of the approaches exploited before used SLNs as the

nanodelivery system. Therefore, in the present work, we have developed a novel approach to functionalize SLNs with Apo E3 in order to mediate the transport and uptake into the brain by a specific event of recognition and binding to LDL receptors. This strategy may allow the whole nanocarrier and the loaded drug to go through the BBB, even passing the drug efflux transporters, promoting a controlled release of the encapsulated drug in the brain (figure 1).

2. Methods

2.1. Materials

For nanoparticle preparation, cetyl palmitate was provided by Gattefossé (Nanterre, France); polysorbate 80 (Tween® 80) was supplied by Merck (Darmstadt, Germany); sodium deoxycholate, avidin, palmitic acid *N*-hydroxysuccinimide ester (NHS-palmitate), *N*-Ethyl-*N'*-(3-Dimethylaminopropyl) carbodiimide hydrochloride, and Apo E3 were provided by Sigma-Aldrich (St. Louis, MO, USA); DSPE-PEG-NH₂ was purchased from Avanti Polar Lipids (Alabaster, AL, USA); and the biotinylation reagent was supplied by Thermo Scientific (Waltham, MA, USA). For the hCMEC/D3 cell culture, endothelial basal medium-2 (EBM-2) was purchased from Lonza (Basel, Switzerland); fetal bovine serum (FBS) 'Gold' was provided by PAA—The Cell Culture Company (Cansera, Canada); chemically defined lipid concentrate and penicillin-streptomycin (PenStrep) were obtained from Gibco (Carlsbad, CA, USA); human basic fibroblast growth factor (bFGF), ascorbic acid, hydrocortisone, and trypsin were purchased from Sigma; ethyl alcohol absolute was supplied by Carlo Erba (Milano, Italy); and Cultrex Rat Collagen I was provided by R&D Systems (Minneapolis, MN, USA).

2.2. Preparation of SLNs

The method chosen for the preparation of the nanoparticles was the high shear homogenization technique [25]. The lipid phase, containing 500 mg of cetyl palmitate (solid lipid) and 150 mg of the stabilizer polysorbate 80, was melted at 70 °C. The molten lipid was then dispersed in 4.35 ml of PBS, pH 7.4, by high-speed stirring (120 s at 12 000 rpm) in an Ultra-Turrax T25 (Janke and Kunkel IKA-Labortechnik, Staufen, Germany) followed by sonication (15 min of 80% intensity) using a Sonics and Materials Vibra-Cell™ CV18 (Newtown, CT, USA). The cooling of the nanoemulsions at room temperature (RT) allowed the crystallization of lipids and subsequent formation of the lipid nanoparticles. The formulations appeared white and milky and had low viscosity. To assess the stability of the formulations, they were stored for six months (RT and protected from light), and the particle size and zeta potential were measured periodically. For the permeability studies, SLNs were labeled with fluorescein isothiocyanate (FITC, 0.4 mg mL⁻¹), which was added to the

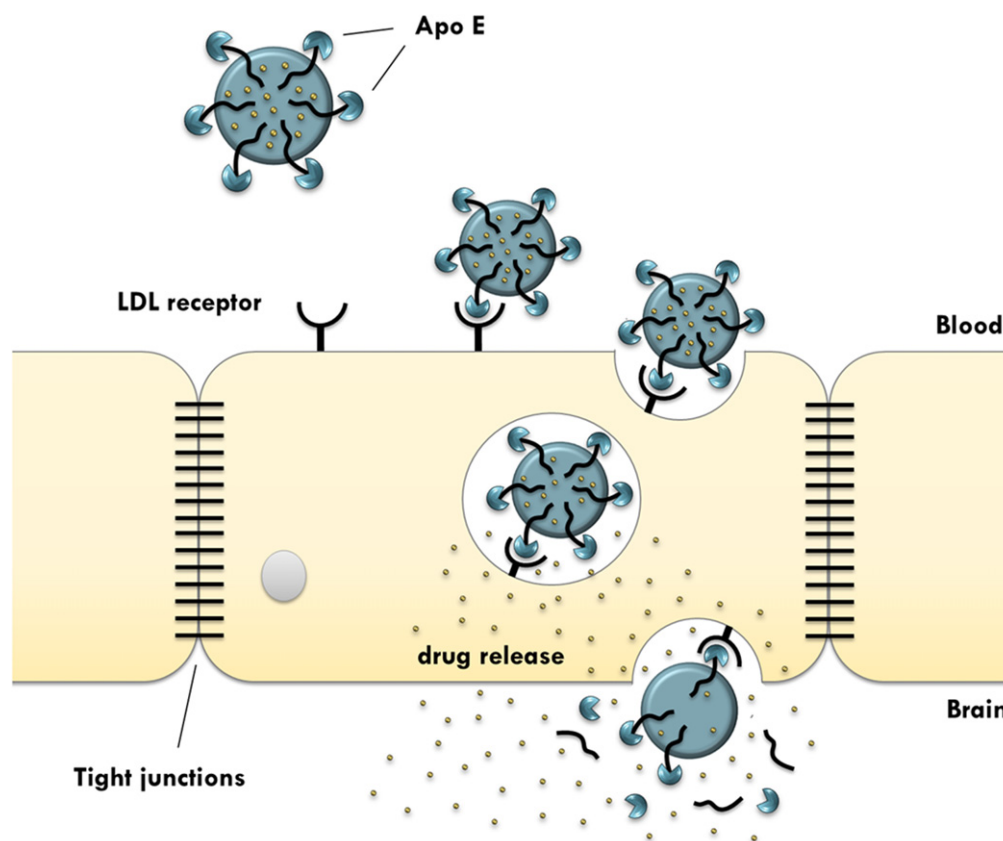


Figure 1. Schematic representation of the proposed mechanism of Apo E-functionalized SLNs' uptake in brain (not to scale).

lipid phase during the SLNs' preparation. The quantification of the loaded dye was assessed indirectly by measuring the free FITC still present in the aqueous phase. Therefore, centrifugal filter devices allowed us to separate the unloaded FITC from the FITC-loaded SLNs, followed by quantification in a Jasco FP-6500 spectrofluorometer (Easton, MD, USA) at 495/521 nm. A loading percentage of 90% was found for FITC, which is satisfactorily high for its use as the fluorescent dye. Moreover, free FITC was excluded by dialysis against PBS overnight in order not to interfere with the SLNs' quantification during the permeability study.

2.3. Nanoparticle functionalization

The main focus of this paper is the development of innovative SLNs functionalized with Apo E, taking advantage of the strongest known non-covalent interaction (K_d of 10^{-15} M) between avidin and biotin. The bond formation between biotin and avidin is very rapid and stable [26]. Therefore, the functionalization of nanoparticles with Apo E started by a previous biotinylation of Apo E, followed by the addition of the functionally active avidins onto the surface of SLNs. This addition was achieved by two different strategies: (i) using DSPE-PEG-Avidin and (ii) using palmitate-avidin conjugated to the nanoparticles. In the first strategy, SLNs were prepared as described above but incorporating 10 mg of DSPE-PEG-NH₂ in their lipid phase composition. Hence, the phospholipid DSPE (1, 2-distearoyl-*sn*-glycero-3-

phosphoethanolamine) was anchored within the lipid matrix of the SLNs, exposing on the surface the terminal amino groups. These nanoparticles were subsequently surface modified by peptide bond formation between the amino groups of the SLNs and the carboxyl groups of avidins (figure S2). Concerning the second strategy, SLNs were prepared as previously described but incorporating a 2 ml solution of palmitate-avidin (5 mg ml^{-1}) in their lipid phase composition. The palmitate preferentially partitioned into the hydrophobic SLNs' matrix, while the hydrophilic avidin was exposed to the surface, creating a modular platform for surface ligand addition (figure S5). The avidin-conjugated nanoparticles then reacted with the previously biotinylated Apo E, producing two different Apo E-functionalized SLNs: SLN-DSPE-ApoE and SLN-Palmitate-ApoE (figure 2). For further detail in the functionalization process, please consult the supporting information material (figures S1–S5).

2.4. Morphology determination

To characterize the morphology of SLNs (with and without functionalization), the nanosystems were observed by transmission electron microscopy (TEM). The samples were mounted on 300 mesh formvar copper grids, stained with uranyl acetate, and examined using a Jeol JEM 1400 TEM microscope (Tokyo). Images were digitally recorded using a Gatan SC 1000 ORIUS CCD camera (Warrendale, PA, USA).

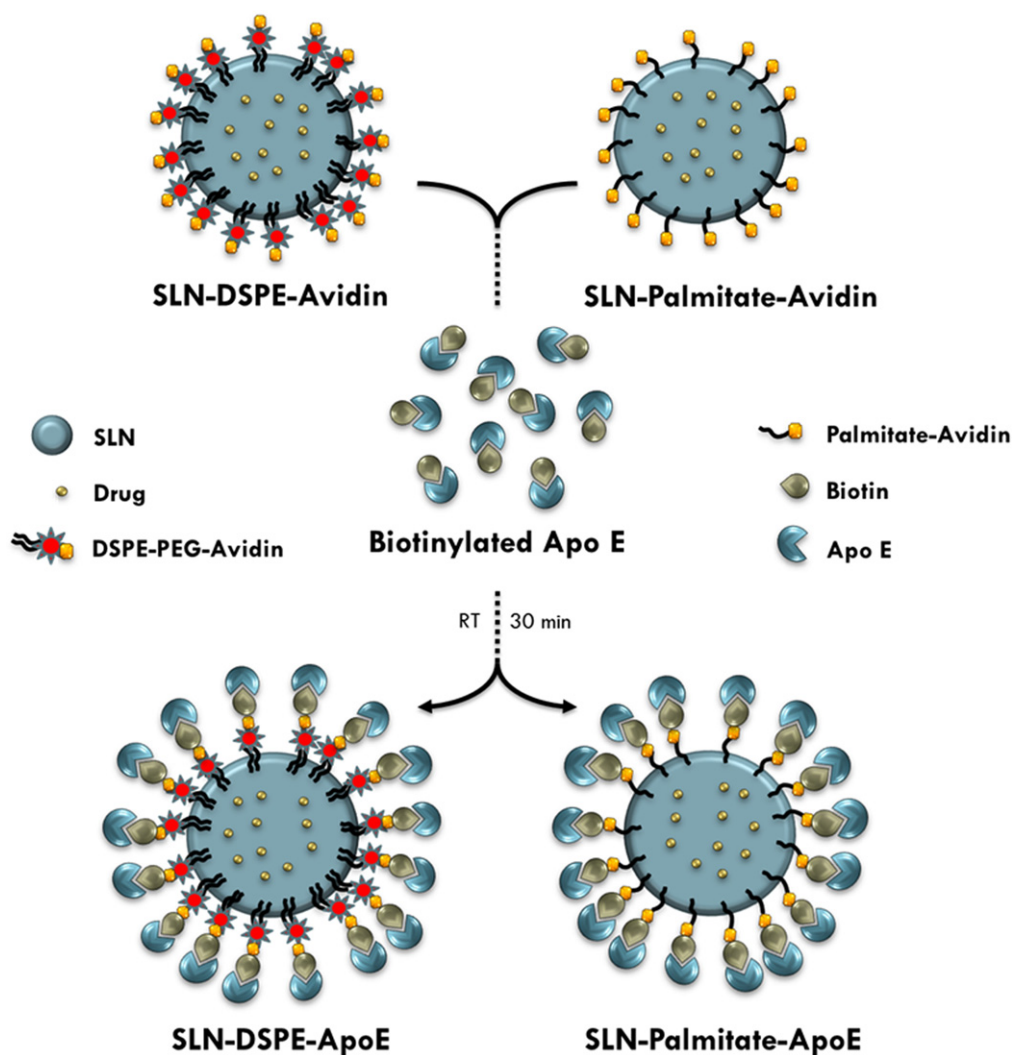


Figure 2. Schematic representation of the addition of biotinylated Apo E to the covalently attached avidin in SLNs, producing two new Apo E-functionalized nanoparticles: SLN-DSPE-ApoE and SLN-palmitate-ApoE (not to scale).

2.5. Particle size and zeta potential measurements

Particle size and zeta potential analysis was performed by dynamic light scattering (DLS) and electrophoretic light scattering (ELS) using Brookhaven Instruments (Holtville, NY, USA). The samples in PBS were analyzed at RT, with a fixed light incidence angle of 90° and an average count rate between 100–500 kcps. The measurements were always performed in triplicate by calculating the average of 10 runs. The DLS technique gives information about the mean hydrodynamic size (Z-average) and the polydispersity index (PDI) of the nanoparticles in suspension. ELS is a technique to measure the electrophoretic mobility and, consequently, the zeta potential of a sample.

2.6. Lyophilization

Samples of SLNs (with and without functionalization) were lyophilized using an Advantage 2.0 bench-top freeze dryer (SP Scientific, Warminster, PA, USA). This process was solely employed in order to use the samples in infrared

spectroscopy experiments, because otherwise the water bands (OH vibrations) could mask the ones related to the sample itself. Firstly, samples were prepared with Aerosil 2% (m/m) as a cryoprotectant. The lyophilization process started by freezing the samples at -60°C , in vacuum, for a period of 720 min. Condensation was made at -80°C under 150 mTorr of pressure. The samples were then dried at 20°C for 1200 min under 150 mTorr. Finally, a secondary drying step was performed at 25°C for 1200 min at 100 mTorr.

2.7. Fourier transform infrared spectroscopy

In order to confirm the presence of Apo E in the functionalized SLNs we performed infrared spectra analysis on the lyophilized samples using Fourier transform infrared spectroscopy (FTIR). By analyzing the absorption bands in the infrared spectrum it is possible to identify vibrational modes associated with certain functional groups of the molecules. Infrared spectra were recorded using a Frontier FTIR Spectrometer from PerkinElmer (Santa Clara, CA, USA) equipped with a DTGS detector and a PIKE Technologies Gladi

attenuated total reflectance (ATR) accessory. Each spectrum was collected as the average of 32 scans with 4 cm^{-1} resolution over a wave number interval between $600\text{--}4000\text{ cm}^{-1}$. Each sample was analyzed in triplicate, and the spectral average was considered for further analysis.

2.8. Fluorimetric assay

In addition to the infrared spectra, fluorimetric assays were also performed to confirm the Apo E-functionalization of the SLNs. For this purpose, a biotinylated fluorescein was used to quantify the available biotin-binding sites on the SLNs through the strong quenching associated to the binding of this probe to the free avidin sites on the nanoparticle surface. Briefly, $5\ \mu\text{l}$ of SLN samples were diluted in 2 ml of PBS and incubated with $5\ \mu\text{l}$ of biotinylated fluorescein at 200 mg ml^{-1} during 30 min, at RT, in order to promote the interaction between the biotin of the probe and the free avidin that exists on the SLN's surface. Then, the samples were transferred into Amicon® Ultra-4 centrifugal filter devices with a 100 nm filter (Millipore, Billerica, MA, USA) and centrifuged using a Jouan BR4i multifunction centrifuge with a KeyWrite-D™ interface (Thermo Electron, Waltham, MA, USA) with a fixed 23° -angle rotor and 4300 rpm spin for 5 min. Sample supernatants were then collected and their fluorescence measured in a Jasco FP-6500 spectrofluorometer (Easton, MD, USA) at wavelength 496/518 nm. The biotinylated fluorescein was used as the positive control in this assay, and the SLN solution with no incubation with the fluorescent probe was used as the negative control.

2.9. hCMEC/D3 cell culture

Immortalized hCMEC/D3 cells until passage number 35 were obtained from the Institut National de la Santé et de la Recherche Médicale (INSERM, Paris, France). This cell line represents a model of the human BBB that can be easily grown and is very useful for the characterization of the interactions between drugs or formulations and brain endothelial cells [27, 28]. Cells were seeded in a concentration of $2.5 \times 10^4\text{ cells/cm}^2$ and grown at 37°C in an atmosphere of 5% CO_2 in EBM-2 medium supplemented with 1% of Pen-Strep, 2% of FBS 'Gold,' 1% of chemically defined lipid concentrate, ascorbic acid at a concentration of $5\ \mu\text{g ml}^{-1}$, hydrocortisone at $1.4\ \mu\text{M}$, HEPES to a final concentration of 10 mM, and bFGF at $1\ \text{ng ml}^{-1}$. This last supplement was added extemporaneously in the culture medium. The cell counting was performed in a Neubauer chamber using the trypan blue exclusion technique, which allowed excluding the damaged dead cells.

2.10. MTT assay

To access the cell viability after SLN exposure, an MTT assay was performed [29]. Cells were seeded in a 96-well plate (10^4 cells per well) pre-coated with type I collagen and grown at 37°C in an atmosphere of 5% CO_2 in a supplemented EBM-2 medium. After 20 h cells were incubated with different concentrations of SLNs (functionalized and non-functionalized)

for 4 h. SLN formulations were previously filtrated through $0.2\ \mu\text{m}$ sterile filter units in order to maintain sterile conditions and minimize contaminations. The medium of each well was separated from the cells and stored for LDH assay, and cells were treated with $0.5\ \text{mg ml}^{-1}$ of MTT for 4 h, at 37°C , 5% CO_2 . Finally DMSO was added to dissolve MTT formazan and incubated for 15 min at 37°C , followed by a measure of absorbance at 550 and 690 nm. Cell viability was expressed as a percentage compared to the cells incubated only with EBM-2 medium (positive control). Triton X-100 was used in the MTT assay as the negative control, since the detergent action disrupts the cells.

2.11. LDH assay

The LDH assay was performed to access cytotoxicity after SLN exposure. The medium resulting from the incubation of SLNs with cells was centrifuged (250 g, 10 min, at RT) and the supernatant separated from the deposited cells in each well. This centrifugation process allowed us to remove any wastes and cellular debris and also SLNs. The LDH release into culture supernatants was detected by adding catalyst and dye solutions of an LDH cytotoxicity detection kit (Takara Bio Inc., Shiga, Japan). The absorbance values were read at 490 nm and 690 nm. Cytotoxicity was expressed as a percentage compared to the maximum LDH release in the presence of triton X-100 (positive control). EBM-2 medium was used in the LDH assay as the negative control, since no cytotoxicity was detected in such conditions.

2.12. Transwell permeability studies

hCMEC/D3 cells were seeded on transwell filters (six-well polyester, pore size $0.4\ \mu\text{m}$ and a diameter of 4.67 cm^2) pre-coated with type I collagen in a density of 2×10^5 cells per insert. A permeability assay was performed 7 d after seeding. Lucifer Yellow (LY) at a concentration of $20\ \mu\text{M}$ was used with a known and reported effective permeability coefficient (P_{eff}) of $1.33 \times 10^{-3}\text{ cm/min}$ for this cell line [30]. The P_{eff} of LY in our studies was verified, comparing the permeability in the monolayer and the permeability in empty filters, where PS is the permeability x surface area product [31]:

$$\frac{1}{PS_{\text{eff}}} = \frac{1}{PS_{\text{with cells}}} - \frac{1}{PS_{\text{without cells}}}$$

The P_{eff} (cm/min) value could be generated by dividing the PS_{eff} by the surface area (A) of the porous membrane:

$$P_{\text{eff}}\ (\text{cm}/\text{min}) = \frac{PS_{\text{eff}}}{A}$$

For the permeability studies, functionalized and non-functionalized SLNs ($1500\ \mu\text{g ml}^{-1}$ of formulation) loaded with FITC ($0.4\ \text{mg ml}^{-1}$) were incubated in the apical donor compartment for 4 h at 37°C in a 5% CO_2 atmosphere. The total amount of FITC in the receptor compartment was quantified after 30, 60, 90, 120, 150, 210, and 240 min by fluorescence analysis (495/519 nm), and the apparent

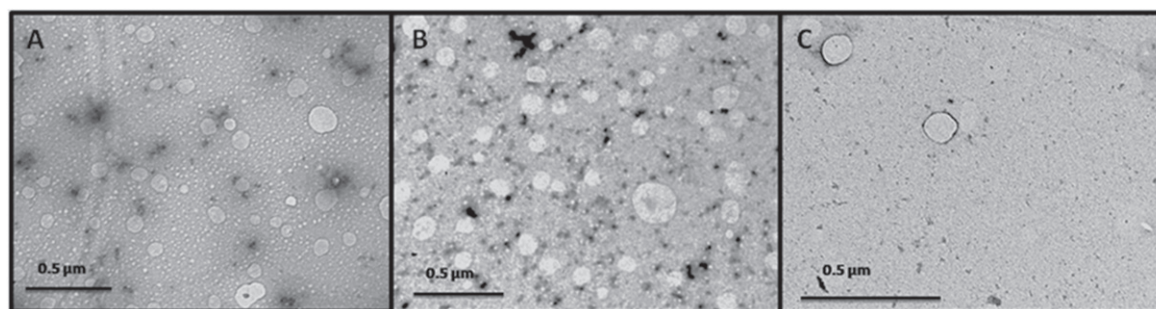


Figure 3. TEM images of SLNs: (A) non-functionalized SLNs; (B) SLN-DSPE-ApoE; and (C) SLN-palmitate-Apo E at 20 000x magnification.

Table 1. Characterization of SLNs non-functionalized; SLNs functionalized with avidin (SLN-DSPE-avidin and SLN-palmitate-avidin); and functionalized with Apo E (SLN-DSPE-ApoE and SLN-palmitate-ApoE).

Formulation Code	Z-average (nm)	PDI	Zeta Potential (mV)
SLNs non-functionalized	151 ± 12	0.19 ± 0.06	-12.5 ± 2.8
SLN-DSPE-Avidin	169 ± 41	0.17 ± 0.09	-9.9 ± 2.7
SLN-DSPE-ApoE	167 ± 27	0.16 ± 0.06	-10.9 ± 1.7
SLN-Palmitate-Avidin	195 ± 15*	0.14 ± 0.04	-12.2 ± 0.3
SLN-Palmitate-ApoE	192 ± 13*	0.14 ± 0.11	-14.6 ± 1.1

Note: All values represent the mean ± standard deviation ($n = 3$). Results of functionalized SLNs were analyzed and compared with non-functionalized SLNs. (*) denotes statistically significant differences ($P < 0.05$).

permeability coefficients (P_{app}) of the SLNs were calculated according to:

$$P_{app}(\text{cm s}^{-1}) = \frac{Q}{A \times C \times t}$$

where Q represents the total amount of permeated FITC (μg) in each time point, A is the surface area of the filter (cm^2), C is the initial FITC concentration ($\mu\text{g cm}^{-3}$), and t is the experiment time (s). The cumulative permeability percentage was also calculated considering the following equation:

$$\% \text{ of permeability} = \frac{|FITC|_{\text{receptor}, t_n}}{|FITC|_{\text{donor}, t_0}} \times 100$$

2.13. Statistical analysis

Statistical analyses were performed using SPSS software (v 20.0; IBM, Armonk, NY, USA). The measurements were repeated at least three times, and data were expressed as mean ± SD. Data were analyzed using one-way analysis of variance (one-way ANOVA), followed by Bonferroni, Tukey, and Dunnett post-hoc tests. A p value less than 0.05 was considered statistically significant.

3. Results

3.1. Morphology determination

The morphology of SLNs with and without functionalization was observed by TEM (figure 3). The images reveal that

SLNs are almost spherical and uniform in shape. It is possible to see particles, mainly in the range of 100–200 nm or smaller, and there is no visible aggregation or agglomeration of particles. Apparently, functionalized SLNs using palmitate have an average size greater than the functionalized SLNs using DSPE. Undoubtedly, for all formulations the most frequent population of particles has a diameter less than 200 nm.

3.2. Particle size and zeta potential measurements

The particle size and surface charge of nanoparticles represent the two most important factors determining the capacity to cross the BBB. Functionalized and non-functionalized nanoparticles were characterized by DLS to verify whether the surface modification of SLNs affected the mean diameter of the particles. The Z-average and PDI of the lipid nanoparticles measured by DLS are presented in table 1. All SLNs showed a homogenous size distribution with a mean diameter less than 200 nm. No statistically significant differences were observed ($P > 0.05$) in average size in the functionalization using DSPE. However, the presence of palmitate-avidin in the emulsion slightly increased the size of the particles. The SLNs functionalized using DSPE have a Z-average lower than 170 nm, and SLNs functionalized using palmitate show a Z-average slightly smaller than 200 nm. Therefore, the functionalized SLNs developed here exhibit an ideal size for brain targeting and increased blood circulation time. In fact, most of the successfully used nanoparticles for the transport of drugs across the BBB present a size ranging from 150–300 nm [32]. Furthermore, PDI values obtained for all formulations were lower than 0.2 (table 1), suggesting low variability and no

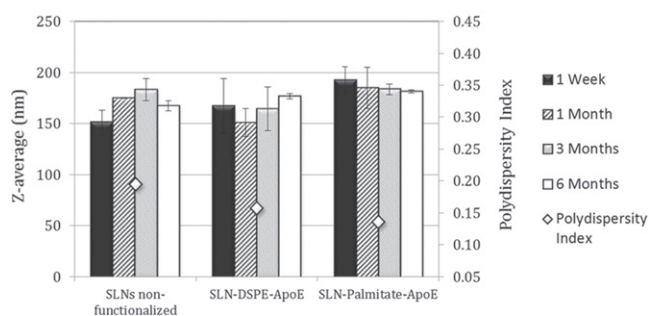


Figure 4. Effect of time of storage on particle size of Apo E-functionalized SLNs compared to non-functionalized SLNs. Note: Z-average after 1 week (■), 1 month (▨), 3 months (▩), 6 months (□), and PDI (◇). All data represent the mean \pm SD ($n = 3$) for three different batches prepared and characterized on separate days. No statistically significant differences were observed over time for any formulation ($P > 0.05$).

aggregation. Looking at zeta potential results in table 1, all formulations presented a negative zeta potential between -10 mV and -15 mV, a value reasonably high to prevent aggregation of nanoparticles. The addition of Apo E to the SLNs did not significantly change this parameter, even though there is a slight increase in the negative zeta potential of the SLNs functionalized using palmitate. Since the BBB has a negative charge, positively charged carriers would be expected to be more efficient in drug delivery to the brain. However, the strong cell binding may prevent the permeation across the barrier [33]. On the other hand, anionic SLNs are able to permeate the BBB without damage to the endothelium with efficient uptake rates [32, 33]. Hence, the lipid nanoparticles developed in the present work are physically stable due to the electrostatic repulsion conferred by the chemical nature of the lipid matrix.

3.3. Stability study

In order to evaluate the stability over time, each formulation was further studied over six months. The physical stability of SLNs in PBS was evaluated, examining changes in the Z-average and zeta potential during storage conditions (25°C and protected from light). For both types of functionalization and for non-functionalized SLNs, the Z-average does not change significantly over time ($p > 0.05$), indicating that there was no aggregation of particles and that they were stable in suspension at least for six months (figure 4). The physical stability of the lipid nanoparticles was also verified periodically by analyzing variations in zeta potential, which is a key factor (figure 5). No statistically significant changes in the zeta potential of functionalized SLNs were verified after six months, suggesting that the surface charge of the particles does not change over time.

3.4. Fourier transform infrared spectroscopy (FTIR)

In order to assess and confirm if the functionalization was successfully developed and to verify the presence of Apo E in SLN formulations, the infrared spectra for each sample were

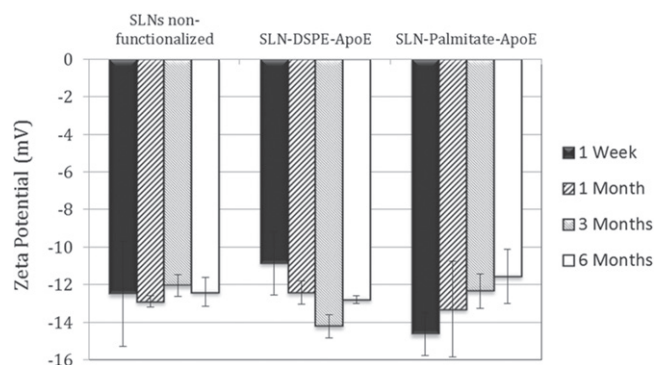


Figure 5. Effect of time of storage on zeta potential of Apo E-functionalized SLNs compared to non-functionalized SLNs. Note: Zeta potential after 1 week (■), 1 month (▨), 3 months (▩), and 6 months (□). All data represent the mean \pm SD ($n = 3$) for three different batches prepared and characterized on separate days. No statistically significant differences were observed over time for any formulation ($P > 0.05$).

collected by FTIR. This technique makes it possible to identify functional groups, which led to the detection and identification of avidin and Apo E molecules in the formulations. A preliminary approach consisted in demonstrating the presence of avidin protein in the particles SLN-palmitate-avidin (figure S6) and SLN-DSPE-avidin (figure S7) for subsequent functionalization with Apo E. In the avidin-functionalized SLNs, but not in the non-functionalized ones, we can easily find three main bands demonstrating the presence of avidin. These bands match to the $-\text{N}-\text{H}$ and $-\text{C}=\text{O}$ groups that exist in the peptide bonds between amino acids that form avidin. The band at 1550 cm^{-1} corresponds to the bending vibrations of $-\text{N}-\text{H}$, the band at 1650 cm^{-1} represents the stretching vibrations of $-\text{C}=\text{O}$, and the other band, not so evident at 3300 cm^{-1} , regards the stretching vibrations of the $-\text{N}-\text{H}$ group. In SLN-palmitate-Apo E (figure S8) and SLN-DSPE-Apo E (figure 6), it is possible to confirm the presence of Apo E after SLN functionalization. In both strategies of Apo E functionalization, two distinct bands are present that are not present in non-functionalized SLNs. One band at 800 cm^{-1} corresponds to the stretching vibrations of $-\text{C}-\text{S}$ bonds only present in biotin, and the other band at 1050 cm^{-1} represents the stretching vibrations of $-\text{C}-\text{N}$ bonds that are greatly increased in the presence of biotin. In this case we can prove the presence of Apo E in the functionalized SLNs by the existence of the biotin molecules connected to Apo E (biotinylated Apo E).

3.5. Fluorimetric assay

In addition to the infrared spectra, fluorimetric assays were also performed to confirm the functionalization of the nanoparticles and to confirm that the biotinylated Apo E is truly linked to the SLNs. For this purpose, we have taken advantage of a biotinylated probe (biotin-fluorescein), which can be used to quantify the available biotin-binding sites in SLNs. As already mentioned, there is a strong quenching phenomenon when the biotin-fluorescein binds to free avidin sites on the

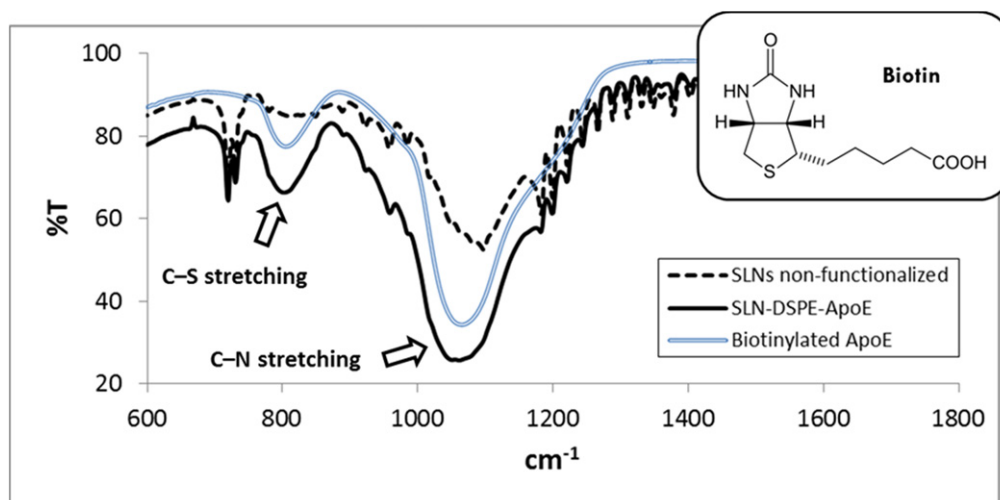


Figure 6. Infrared spectrum obtained by FTIR for SLNs with no functionalization and SLN- DSPE-Apo E. Note: biotinylated Apo E was used as a reference to compare with the functionalized sample.

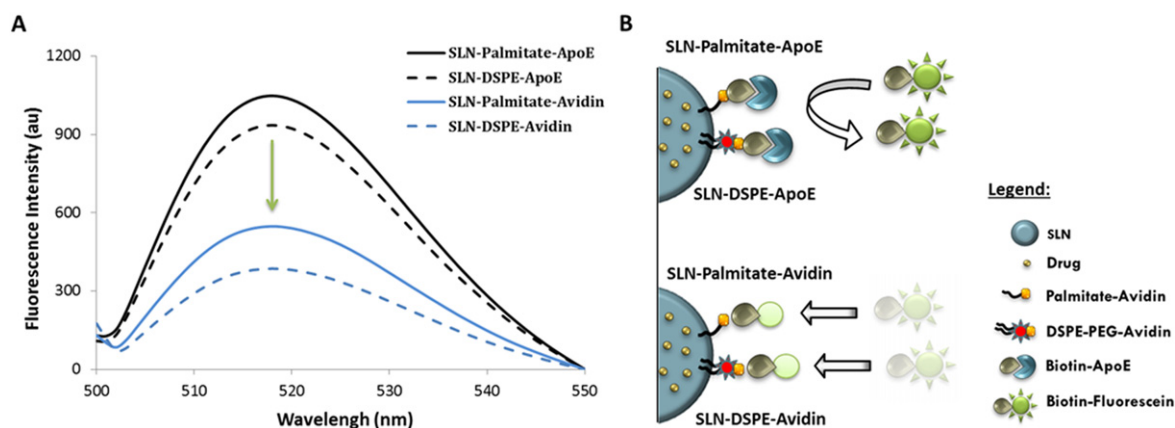


Figure 7. (A) Fluorimetric assay using biotinylated fluorescein to confirm the presence of Apo E in the samples functionalized (—SLN-palmitate-Apo E; - -SLN-DSPE-Apo E). Black lines represent formulations with Apo E and blue lines represent formulations with only avidin (without Apo E linked). (B) Schematic representation of the addition of biotinylated fluorescein to avidin-functionalized SLNs, resulting in the quenching of the fluorescent probe (bottom). In the presence of SLNs functionalized with Apo E, the fluorescein cannot bind to avidin molecules, since they have already been occupied by the biotinylated Apo E, resulting in a maximal fluorescence emission of the probe in solution (above).

surface of the SLNs. So, if the functionalization has been successful, the biotinylated Apo E will be attached to the avidin molecules on SLNs, and there will be few or no binding sites for the probe, resulting in a maximum fluorescence of the fluorescein that is mostly in solution. Therefore, the probe was incubated with samples functionalized with Apo E and samples only functionalized with avidin (without binding Apo E) for comparing the fluorescence obtained. Figure 7 illustrates the results of the fluorimetric assays for both SLN functionalizations with Apo E using palmitate and DSPE. When we have SLNs only functionalized with avidin molecules, there will be many sites for the binding of the biotin-fluorescein probe, resulting in a very sharp decrease in its fluorescence. However, in Apo E-functionalized SLNs there is a more pronounced fluorescence due to the lack of binding sites for the probe that are occupied by the presence of biotinylated Apo E. Therefore, in both strategies of Apo E-functionalization of SLNs (SLN-palmitate-Apo E and SLN-

DSPE-Apo E) we could prove the presence of Apo E linked to the SLNs' surface, because probe fluorescence was substantially higher (two- and three-fold higher, respectively) when compared to SLNs only functionalized with avidin.

3.6. MTT and LDH assays

The *in vitro* cytotoxicity of the developed functionalized SLNs was assessed by cell viability determination and membrane integrity evaluation using the hCMEC/D3 cell line through MTT and LDH assays, respectively. Figure 8 represents the results of the MTT and LDH assays. When cells were exposed to 300 and 1500 $\mu\text{g ml}^{-1}$ of all types of SLNs for 4 h, no changes were observed in MTT metabolism or LDH release when compared to cells exposed to the EBM-2 medium alone, indicating that the SLNs affected neither the metabolic activity of the cells nor the membrane integrity. Only at concentrations of particles equal to or higher

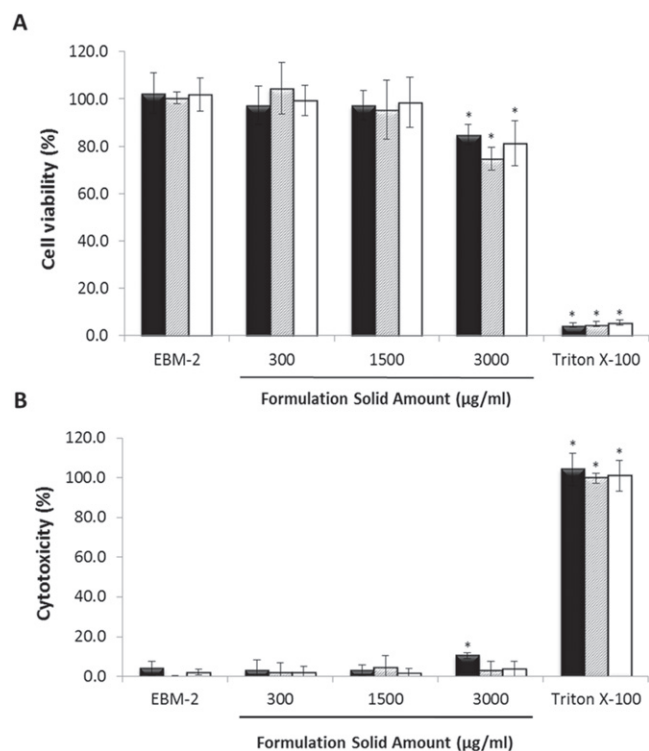


Figure 8. hCMEC/D3 cell viability assessed by MTT assay (A) and cytotoxicity assessed by LDH assay (B) when exposed for 4 h to non-functionalized SLNs (■), functionalized SLN-DSPE-Apo E (▒), and functionalized SLN-palmitate-Apo E (□) at different concentrations (from 300–3000 $\mu\text{g ml}^{-1}$ of solid amount). Note: all values represent the mean \pm standard deviation ($n = 3$). Results of non-functionalized and functionalized SLNs were analyzed and compared with EBM-2 medium, which represents the maximum of cell viability and the minimum of cytotoxicity. (*) denotes statistically significant differences ($P < 0.05$).

than 3000 $\mu\text{g ml}^{-1}$ was any significant reduction observed in the cell metabolic activity. The purpose of verifying the absence of a cytotoxic effect of the developed SLNs on the hCMEC/D3 cell line during 4 h of exposure was also to determine the maximum concentration of SLNs that could be used in permeability studies. Thus a maximum concentration of 1500 $\mu\text{g ml}^{-1}$ could be used without compromising the cell metabolic activity and membrane integrity of the cell barrier. Comparing all formulations, no differences have been found with the Apo E functionalization of SLNs using both strategies, showing good tolerability to the added compounds used for binding Apo E to the SLNs and the safety of the developed delivery systems. In general, a dose-dependent effect is observed, since the effect is more pronounced for higher concentrations. In figure S9, it is possible to see the results of MTT and LDH assays after 24 h incubation of the cells with SLNs, providing further knowledge about the SLNs' cytotoxicity.

3.7. BBB permeability studies

Previously, it has been reported that hCMEC/D3 permeability coefficients were well correlated with *in vivo* permeability data, so transwell devices were cultured with hCMEC/

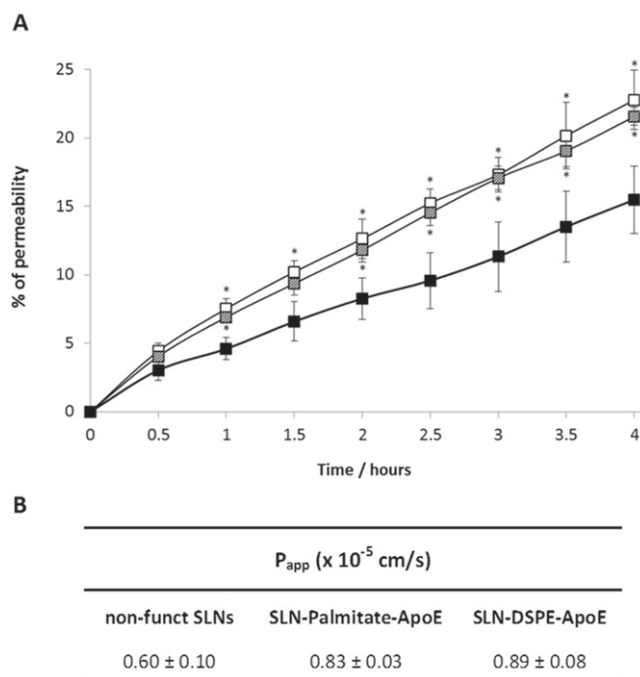


Figure 9. (A) Permeability profile and (B) apparent permeability (P_{app}) values of non-functionalized SLNs (■), functionalized SLN-palmitate-Apo E (▒), and functionalized SLN-DSPE-Apo E (□) after 4 h of transport across the hCMEC/D3 cell monolayer, mimicking BBB permeability conditions. Note: all values represent the mean \pm standard deviation ($n = 3$). Results of functionalized SLNs were analyzed and compared with non-functionalized SLNs. (*) denotes statistically significant differences ($P < 0.05$).

D3 cells, and permeability studies were performed in order to predict the permeability of the formulations developed in the BBB [27]. LY was used as reference at a concentration of 20 μM , and its P_{eff} was determined over a 1 h transport experiment in the presence and in the absence of SLNs. The P_{eff} of LY was found to be $1.32 \pm 0.07 \times 10^{-3} \text{ cm/min}$ in the absence or in the presence of SLNs, which is in agreement with the literature value of $1.33 \times 10^{-3} \text{ cm/min}$, showing the proper confluence of the monolayer for the assays performed with the SLNs developed in this work [30]. At the same time, this information proves that SLNs are not toxic to the monolayer, complementing the results of the MTT and LDH assays. In figure S10, it is also possible to see that the hCMEC/D3 monolayer maintains its integrity with no relevant morphological changes after the assay. The permeability results for each formulation during time can be seen in figure 9. The addition of Apo E (active brain ligand) significantly increased the P_{app} of SLNs after 4 h of transport across the hCMEC/D3 cell monolayer, reaching a value of $0.83 \pm 0.03 \times 10^{-5} \text{ cm s}^{-1}$ for SLN-palmitate-Apo E and $0.89 \pm 0.08 \times 10^{-5} \text{ cm s}^{-1}$ for SLN-DSPE-Apo E, permeabilities 1.5-fold higher than for non-functionalized SLNs with a P_{app} of $0.60 \pm 0.10 \times 10^{-5} \text{ cm s}^{-1}$. The difference between the two strategies of functionalization was not statistically significant, suggesting that Apo E binds properly to SLNs and can carry the SLNs across the monolayer with an

incremented permeability, resulting in active targeting in both strategies.

4. Discussion

Despite enormous efforts in the development of new drugs for brain diseases, few drugs have entered the market, reflecting the complexity of the CNS and the difficulty of crossing the BBB to reach the brain [2, 4]. Nanotechnology has emerged as an area of research for improving and overcoming this difficulty [5, 7]. The potentiality of incorporating both lipophilic and hydrophilic molecules, coupled to the possibility of several administration routes, makes SLNs a very promising delivery system [1, 8, 9]. These nanoparticles open a new window for an effective delivery of a vast variety of drugs, including analgesics and anticancer, anti-aging, or antibiotic agents into the brain, improving their pharmacokinetic profile and allowing higher concentrations to be attained in the brain. There have been some studies describing the preparation of nanoparticles adsorbing Apo E molecules on their surface [15, 16]. Moreover, albumin nanoparticles have already been conjugated with Apo E, aiming to enhance their binding to LDL receptors on the brain endothelial cells to improve the affinity for the BBB [18, 19]. In the present study, we have created a new system using SLNs with a specific linkage to Apo E molecules and taking advantage of the strong interaction between biotin and avidin. These innovative systems were prepared using two strategies of functionalization with Apo E (SLN-DSPE-Apo E and SLN-palmitate-Apo E), producing highly effective drug carriers. As a result, both systems presented spherical and uniform-shaped nanoparticles with an average size below 200 nm and a reasonably negative zeta potential between -10 mV and -15 mV. Also, a quite appealing feature of these systems is their high physical stability, since no changes in these parameters were reported over six months, indicating a good stability of the Apo E-functionalized SLNs. Moreover, the functionalization of SLNs with Apo E was clearly demonstrated by infrared spectra and through fluorimetric assays for both strategies of functionalization (using DSPE or palmitate as the linker molecule). The *in vitro* cell viability and cytotoxicity assays indicated very low cell toxicity when hCMEC/D3 cells were exposed to the SLNs (either functionalized and non-functionalized ones). Permeability studies performed in transwell devices revealed a statistically significant increase of ApoE-functionalized SLN uptake (1.5-fold higher) when compared to SLNs with no functionalization. This allowed us to conclude that Apo E bound properly to SLNs in both functionalization strategies and could carry SLNs across the BBB, promoting an active target.

5. Conclusions

Two new strategies of SLN functionalization with Apo E were quite successfully developed and are very promising for drug delivery into the brain. SLNs were characterized

according to their morphology, average size (<200 nm), low polydispersity (<0.2), zeta potential (between -10 mV and -15 mV), and good stability at storage conditions. The functionalization of SLNs with Apo E was successfully verified by infrared spectroscopy and fluorimetric assays. The *in vitro* validation of ApoE-functionalized SLNs was performed in hCMEC/D3 cells, revealing no toxicity and a 1.5-fold increment in the BBB permeability. Therefore, these new systems may constitute a promising strategy for brain targeting, since Apo E-functionalized SLNs may mimic lipoprotein particles, crossing the BBB endothelium into the brain.

Acknowledgments

This work received financial support from National Funds (FCT, Fundação para a Ciência e a Tecnologia) through project Pest-C/EQB/LA0006/2013. The work also received financial support from the European Union (FEDER funds) under the framework of QREN through Project NORTE-07-0124-FEDER-000067. To all financing sources the authors are greatly indebted. ARN also acknowledges the FCT for financial support through the PhD grant SFRH/BD/73379/2010. We are also grateful to Dr. Rui Fernandes (IBMC) for expert help with TEM.

References

- [1] Kaur I P *et al* 2008 Potential of solid lipid nanoparticles in brain targeting *J. Control. Release* **127** 97–109
- [2] Abbott N J *et al* 2010 Structure and function of the blood-brain barrier *Neurobiol. Dis.* **37** 13–25
- [3] Sahni J K *et al* 2011 Neurotherapeutic applications of nanoparticles in Alzheimer's disease *J. Control. Release* **152** 208–31
- [4] Pardridge W M 2002 Why is the global CNS pharmaceutical market so under-penetrated? *Drug Discov. Today* **7** 5–7
- [5] Wong H L, Wu X Y and Bendayan R 2012 Nanotechnological advances for the delivery of CNS therapeutics *Adv. Drug Deliv. Rev.* **64** 686–700
- [6] Wong H L *et al* 2010 Nanotechnology applications for improved delivery of antiretroviral drugs to the brain *Adv. Drug Deliv. Rev.* **62** 503–17
- [7] Alam M I *et al* 2010 Strategy for effective brain drug delivery *Eur. J. Pharm. Sci.* **40** 385–403
- [8] Rostami E *et al* 2014 Drug targeting using solid lipid nanoparticles *Chem. Phys. Lipids* **181** 56–61
- [9] Blasi P *et al* 2007 Solid lipid nanoparticles for targeted brain drug delivery *Adv. Drug Deliv. Rev.* **59** 454–77
- [10] Muller R H *et al* 1997 Cytotoxicity of solid lipid nanoparticles as a function of the lipid matrix and the surfactant *Pharm. Res.* **14** 458–62
- [11] Chattopadhyay N *et al* 2008 Solid lipid nanoparticles enhance the delivery of the HIV protease inhibitor, atazanavir, by a human brain endothelial cell line *Pharm. Res.* **25** 2262–71
- [12] Kreuter J 2005 Application of nanoparticles for the delivery of drugs to the brain *Int. Congress Ser.* **1277** 85–94
- [13] Rempe R *et al* 2011 Transport of Poly(n-butylcyano-acrylate) nanoparticles across the blood-brain barrier *in vitro* and their influence on barrier integrity *Biochem. Biophys. Res. Commun.* **406** 64–9

- [14] Estella-Hermoso de Mendoza A *et al* 2011 *In vitro* and *in vivo* efficacy of edelfosine-loaded lipid nanoparticles against glioma *J. Control. Release* **156** 421–6
- [15] Prabhakar K *et al* 2013 Tween 80 containing lipid nanoemulsions for delivery of indinavir to brain *Acta Pharm. Sinica B* **3** 345–53
- [16] Goppert T M and Muller R H 2005 Polysorbate-stabilized solid lipid nanoparticles as colloidal carriers for intravenous targeting of drugs to the brain: comparison of plasma protein adsorption patterns *J. Drug Target* **13** 179–87
- [17] Chen Y and Liu L 2012 Modern methods for delivery of drugs across the blood-brain barrier *Adv. Drug Deliv. Rev.* **64** 640–65
- [18] Zensi A *et al* 2009 Albumin nanoparticles targeted with Apo E enter the CNS by transcytosis and are delivered to neurones *J. Control. Release* **137** 78–86
- [19] Wagner S *et al* 2012 Uptake mechanism of ApoE-modified nanoparticles on brain capillary endothelial cells as a blood-brain barrier model *PLoS One* **7** e32568
- [20] Kim D H *et al* 1996 Human apolipoprotein E receptor 2. A novel lipoprotein receptor of the low density lipoprotein receptor family predominantly expressed in brain *J. Biol. Chem.* **271** 8373–80
- [21] Dehouck B *et al* 1994 Upregulation of the low density lipoprotein receptor at the blood-brain barrier: intercommunications between brain capillary endothelial cells and astrocytes *J. Cell Biol.* **126** 465–73
- [22] Hauser P S, Narayanaswami V and Ryan R O 2011 Apolipoprotein E: from lipid transport to neurobiology *Prog. Lipid Res.* **50** 62–74
- [23] Michaelis K *et al* 2006 Covalent linkage of apolipoprotein e to albumin nanoparticles strongly enhances drug transport into the brain *J. Pharmacol. Exp. Ther.* **317** 1246–53
- [24] Hoffmann M *et al* 2001 Diminished LDL receptor and high heparin binding of apolipoprotein E2 Sendai associated with lipoprotein glomerulopathy *J. Am. Soc. Nephrol.* **12** 524–30
- [25] Neves A R *et al* 2013 Novel resveratrol nanodelivery systems based on lipid nanoparticles to enhance its oral bioavailability *Int. J. Nanomed.* **8** 177–87
- [26] Lesch H P *et al* 2010 Avidin-biotin technology in targeted therapy *Expert Opin. Drug Deliv.* **7** 551–64
- [27] Weksler B B *et al* 2005 Blood-brain barrier-specific properties of a human adult brain endothelial cell line *FASEB J.* **19** 1872–4
- [28] Weksler B, Romero I A and Couraud P O 2013 The hCMEC/D3 cell line as a model of the human blood brain barrier *Fluids Barriers CNS* **10** 16
- [29] Mosmann T 1983 Rapid colorimetric assay for cellular growth and survival: application to proliferation and cytotoxicity assays *J. Immunol. Methods* **65** 55–63
- [30] Poller B *et al* 2008 The human brain endothelial cell line hCMEC/D3 as a human blood-brain barrier model for drug transport studies *J. Neurochem.* **107** 1358–68
- [31] Cecchelli R *et al* 1999 *In vitro* model for evaluating drug transport across the blood-brain barrier *Adv. Drug Deliv. Rev.* **36** 165–78
- [32] Wohlfart S, Gelperina S and Kreuter J 2012 Transport of drugs across the blood-brain barrier by nanoparticles *J. Control. Release* **161** 264–73
- [33] Lockman P R *et al* 2004 Nanoparticle surface charges alter blood-brain barrier integrity and permeability *J. Drug Target* **12** 635–41